ELSEVIER

Polymer 43 (2002) 2795–2802

polymer

www.elsevier.com/locate/polymer

Strain rate effects in polycarbonate and polycarbonate/ABS blends

J.P.F. Inberg[1], A. Takens[2], R.J. Gaymans*

Laboratory of Polymer Technology, Department of Chemical Technology, Faculty of Chemical Technology, University of Twente, P.O. Box 217, 7500 AE Enschede, The Netherlands

Received 25 April 2001; received in revised form 2 January 2002; accepted 11 January 2002

Abstract

Acrylonitrile–butadiene–styrene was blended in polycarbonate using a twin-screw extruder, producing dispersed and co-continuous blends. The blends were injection moulded into test bars. These materials were tested in single edge notch tensile tests as a function of test speed over a test speed range of 10^{-4}–10 m s^{-1} (2.85×10^{-3}–2.85×10^{2} s^{-1}). Infrared measurements were made to monitor the temperature development in the material during fracture. The fracture energies were higher at high test speeds than could be expected based on the low speeds results. This effect was due to an increased fracture stress, initiation strain, and propagation strain. With infrared measurements a temperature increase of 30–40 °C was observed. Also the size of the deformation zone increased with test speed. A possible explanation is a thermal blunting resulting from adiabatic heating at high speeds. The brittle–ductile transition temperature increased linearly with the logarithm of the strain rate by a factor of 18.6. At high test speeds the brittle–ductile transition developed with the formation of shear lips.

Keywords: Polycarbonate; Acrylonitrile–butadiene–styrene; Strain rate

1. Introduction

Yield behaviour of polymers is affected by temperature and strain rate, as described by the Eyring equation:

$$\sigma_{yT} = \frac{2}{\gamma V}\left[\Delta H - 2.303RT \log\left(\frac{\dot{\varepsilon}_0}{\dot{\varepsilon}}\right)\right] \quad (1)$$

with tensile yield stress σ_{yT}, activation energy ΔH, activation volume V, and gas constant R [1,2]. If a second phase is present, the stress concentration factor, γ, takes into account the dependence of yield stress on second phase content and can be calculated by using the Ishai–Cohen relation [3] $1/\gamma = 1 - 1.21\phi^{2/3}$, where ϕ is the volume fraction of soft particles.

An important parameter in the fracture of semi-ductile polymers is the brittle-to-ductile transition. This transition is described by the Ludwig–Davidenkov–Orowan criterion by looking at the influence of strain rate on yield stress as well as fracture stress (Fig. 1). Yield stress increases with strain rate, more than the fracture stress changes with strain rate. At a certain point, yield stress becomes higher than fracture stress and brittle fracture occurs. Increasing the strain rate and decreasing the temperature leads to the brittle–ductile transition taking place earlier.

The plastic deformation that takes place during the fracture can result in a significant rise in temperature [1,4–8], resulting in a lower draw stress, more deformation and if appropriate crack tip blunting. An estimation of the maximum rise in temperature in the material can be made by using Eq. (2) [9]:

$$\Delta T_{max} = \psi \frac{\varepsilon_b}{2\rho c_p}(\sigma_y + \sigma_b) \quad (2)$$

assuming that deformation is adiabatic and homogeneous in the deformation zone, with yield stress σ_y, fracture stress σ_b, fracture strain ε_b, density ρ, c_p the heat capacity of the material, and ψ the fraction of plastic work that is transformed into heat. Transition from isothermal to adiabatic deformation was calculated to occur between 10^{-4} and 1 m s^{-1} tensile test speed [9], corresponding to a deformation rate of 2.85×10^{-3}–28.5 s^{-1}. Using Eq. (2) the temperature rise in polycarbonate (PC) and PC/ABS can be calculated. If it is assumed that $\psi = 1$ and the fracture strain (as measured in tensile) is about 100% a temperature rise of 40 °C can be expected. At this strain the glass transition temperature of PC (~150 °C) will not be reached. However, the local strains in the fracture zone can be higher than the engineering strains in tensile tests and this will lead to a larger temperature rise in the fracture zone. It can be calculated that the T_g of PC can be reached if the strain is in the order of 350%.

* Corresponding author.
E-mail address: r.j.gaymans@ct.utwente.nl (R.J. Gaymans).
[1] Present address: Wavin b.v., Dedemsvaart, The Netherlands.
[2] Present address: Mattel b.v., Amstelveen, The Netherlands.

0032-3861/02/$ - see front matter
PII: S0032-3861(02)00081-2

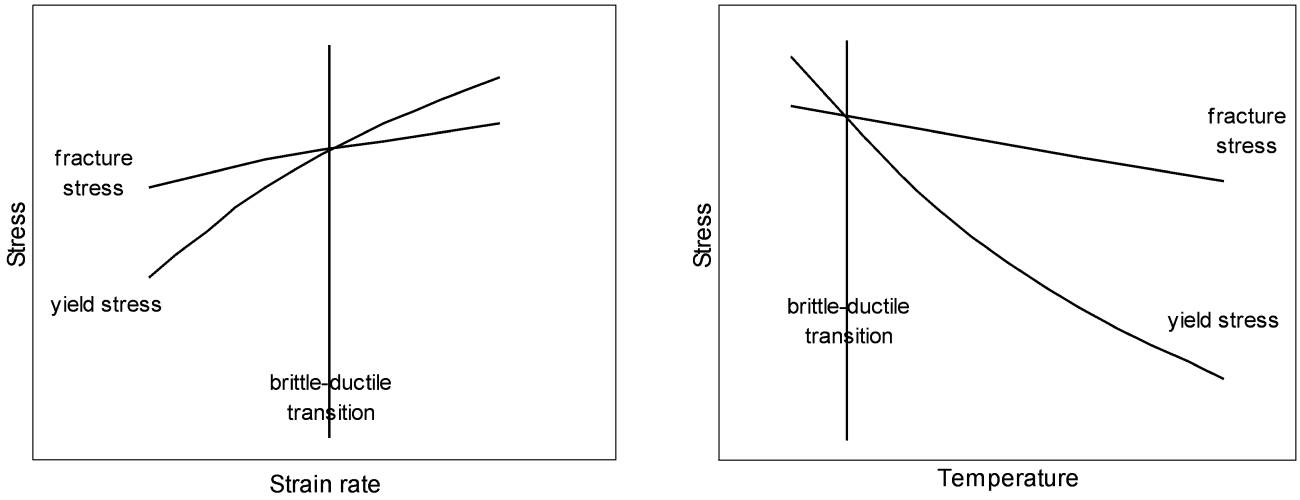

Fig. 1. Ludwig–Davidenkov–Orowan theory describing brittle-to-ductile transition due to (a) strain rate; (b) temperature.

Williams and Hodgkinson [6] studied the fracture toughness G_c over a range of strain rates for HDPE, PTFE, and PMMA. They found a pronounced rate effect on measured toughness and that G_c scaled with loading time, $G_c \propto t^{1/2}$. This effect was explained by adiabatic heating. The consequential softening and crack-tip blunting resulted in an increased toughness at higher strain rates.

Dijkstra et al. [9] studied the effect of strain rate on crack initiation and propagation in rubber-modified nylon-6. They concluded that the high ductility at high test speeds was the result of the material being molten in the fracture zone and this resulted in thermal blunting of the tip. Similar conclusion was drawn for the high fracture energies of PP–rubber blends [10]. Ricco and Pavan [11] studied J_{Ic}-values for nylon-6 over a range of test speeds. They found that J_{Ic} goes through a maximum. This effect was more pronounced with increasing rubber content. An explanation for this phenomenon was not given.

Experimental data for PC and PC/ABS blends over a range of test speeds, including high speed deformation, are rarely found in open literature. Usually test data obtained in low-deformation-rate tests are used for modelling of the high deformation rate behaviour of this and other complex blends. However, based on research results on acrylonitrile–butadiene–styrene (ABS) [12], it is evident that high rate behaviour is by no means an extrapolation of the behaviour at low deformation rates. The influence of test speed on the behaviour of PC and PC/ABS blends is therefore studied in single edge notched tensile (SENT) tests over a wide speed range and temperatures. Both a co-continuous PC/ABS blend and ABS dispersed in PC are studied.

2. Experimental

2.1. Materials

Commercially available PC, SAN, SAN/PB core-shell impact modifier and PC/ABS blend were kindly supplied by DOW Benelux and GE Plastics. The material specifications are listed in Table 1. PC/ABS blends were made to study the behaviour of a co-continuous PC/ABS blend as well as a blend where ABS was dispersed in PC.

2.2. Specimen preparation

Two different types of PC/ABS blends were made, dispersed and co-continuous blends.

Blend I. For the study of dispersed blends, ABS (Cycoloy) material was used (Table 1). PC and ABS (Cycoloy) were blended to produce PC/ABS blends containing 0, 10, and 45% ABS, dispersed in PC. Compounding was done at 140 rpm and barrel temperatures of 245–270 °C.

Blend II. Co-continuous PC/ABS (50/50) was

Table 1
Material properties

Material	Provided by	Description
PC: Lexan HF1110R	GE Plastics	Bisphenol A polycarbonate, density 1.20 g cm^{-3}, MFR = 25 g/10 min
SAN: Tyril 790	DOW Benelux	Styrene acrylonitrile, 29% AN, density 1.08 g cm^{-3}, MFR = 21 g/10 min
PB: GRC 310	DOW Benelux	ABS: SAN grafted PB powder, PB content 50%, particle size 0.1 μm
Cycoloy C1000A	GE Plastics	PC/ABS blend, containing 55% PC, 45% bulk-ABS (1/3 PB, 2/3 SAN), density 1.06 g cm^{-3}, MFR = 15 g/10 min

compounded in two steps using a Berstorff (ZE 25 × 33D) twin-screw extruder. In the first extrusion step at barrel temperatures 185/190/190/190/200/200/200 °C and screw speed 200 rpm, a core shell rubber of polybutadiene with SAN shell (GRC-rubber) was blended into SAN, producing ABS with 15 wt% PB. In the second extrusion step at barrel temperatures of 215/220/220/220/230/230/230 °C and 200 rpm, ABS was blended into PC in a 50/50 weight ratio, producing a co-continuous PC/ABS blend.

After compounding, the blends were injection moulded into rectangular bars of $74 \times 10 \times 4$ mm^3 using an Arburg Allrounder 221-55-250 injection moulding machine. Barrel temperatures were 230 °C for the co-continuous PC/ABS, with mould temperature 80 °C and injection pressure 55 bar at 100 rpm screw speed. For PC and dispersed PC/ABS the barrel temperatures were 270 °C and injection pressure was 40 bar.

A single-edge V-shaped notch of 2 mm depth and tip radius 0.25 mm was milled in the specimens after moulding.

2.3. SENT tests

Notched specimens were fractured at different test speeds in SENT tests. A Schenck VHS servohydraulic tensile test machine was used with clamp speeds of 10^{-4}–10 m s^{-1}. The specimen length between the clamps was 35 mm, resulting in initial strain rates of 2.85×10^{-3}–285 s^{-1}. All measurements were performed in five-fold.

2.4. IR camera

The temperature rise in the specimens during fracture was monitored using an infrared camera. Specifications are listed in Table 2. With the infrared camera, only temperatures at the surface of the specimen can be determined. The spot size of the camera is about 100 μm, which is large compared to the fracture zone size.

3. Results and discussion

SENT tests were used to test materials over the speed range of 10^{-4}–10 m s^{-1}. The resulting initial strain rates were calculated for the notched tensile specimens, using an effective specimen length of 35 mm (Table 3). As the deformation is beyond the yield point inhomogeneous, especially when a notch is present, the strain rates then cannot be obtained so easily. Force and displacement results were monitored and energy results were determined. First results of PC and dispersed PC/ABS blends will be discussed, then the results for the co-continuous blend.

Table 2
Technical data for the infrared camera, equipped with close-up lens (TVS 600 AVIO Nippon Avionics Co., Ltd)

Temperature range	−20 to 300 °C
Temperature resolution	0.15 °C
Spectral range	8–14 μm
Image rate	30 frames s^{-1}
Spatial resolution	0.1 mm spot size

Table 3
Initial deformation rates in SENT test with specimen length of 35 mm between clamps

Clamp speed (m s^{-1})	SENT initial deformation rate (s^{-1})
10	2.85×10^{2}
1	2.85×10^{1}
10^{-1}	2.85
10^{-2}	2.85×10^{-1}
10^{-3}	2.85×10^{-2}
10^{-4}	2.85×10^{-3}

3.1. PC and PC/ABS dispersed

Blend I type materials were studied in SENT tests. PC/ABS blends containing 0, 10, and 45% ABS were used. The blends were tested at room temperature over the test range of 10^{-4}–10 m s^{-1}, resulting in initial strain rates as indicated in Table 3. The 10% blend was tested also at different temperatures. Brittle-to-ductile transition temperatures at various speeds were obtained from these results.

During SENT tests, force and displacement were monitored. Maximum stress is defined as the maximum force measured during the SENT test divided by the cross-sectional area behind the notch. Maximum stress was measured for the dispersed PC/ABS blends as a function of test speed (Fig. 2a). The maximum stress for PC and the PC/ABS blends appeared to increase with test speed. The increase is stronger than can be expected, based on the influence of strain rate on yield stress predicted by the Eyring equation (Eq. (1)). Especially at high test speeds the increase is strong. This effect was also found, more clearly, for ABS [12], PP–rubber blends [10] and nylon-6–rubber blends [9] and explained by an adiabatic temperature rise in the material ahead of the notch, leading to notch tip blunting. The 10% ABS blend behaves similarly to PC over the whole test speed range. The 45% ABS blend has lower maximum stresses but the trend is the same as for PC and the 10% blend.

Fracture propagation displacement is defined as the clamp displacement after fracture is initiated. The propagation displacement for PC decreases with clamp speed and is surprisingly higher for the 1 m s^{-1} test (Fig. 2b). The propagation displacements of the 10 and 45% blends decrease in a similar manner as PC, with values slightly lower than PC. The propagation displacements are only a small part of the total displacement.

With increasing test speed the materials are expected to fracture in a more brittle manner. However, the combination of a higher fracture stress and a slightly lower fracture strain surprisingly resulted in a more ductile behaviour of the material (Fig. 2c). For pure PC, the fracture energy increased with clamp speed up to 1 m s^{-1}, the value at

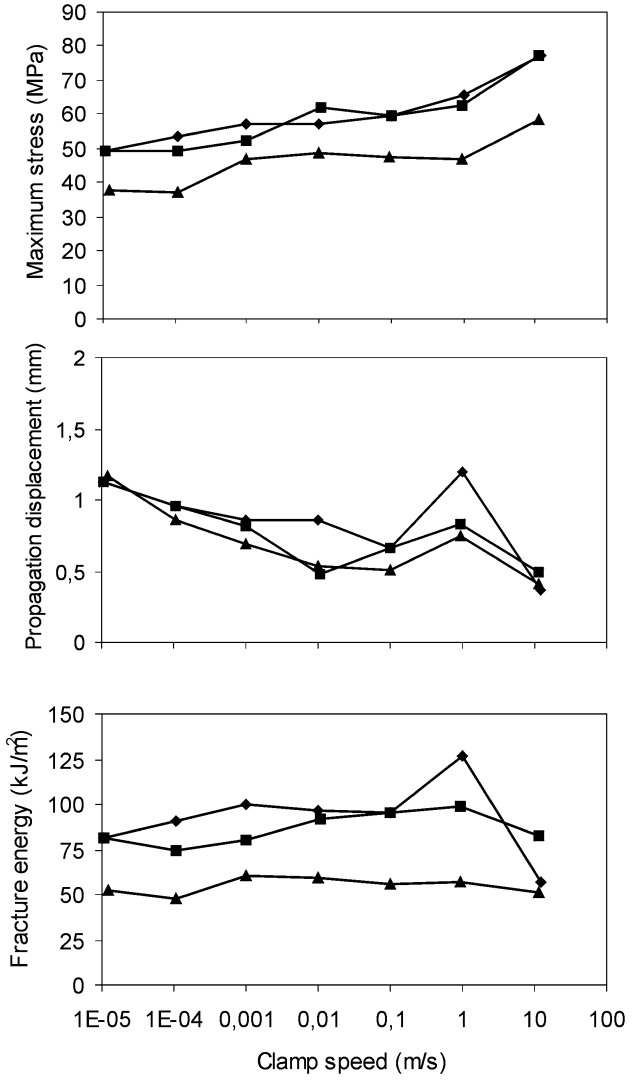

Fig. 2. Influence of test speed on SENT results (maximum stress, fracture displacement, and fracture energy) for dispersed PC/ABS blend (type I), room temperature with different ABS content: (◆) 0%; (■) 10%; (▲) 45%.

1 m s^{-1} being very high. At 10 m s^{-1} the fracture energy is considerably lower as here the fracture type changed to brittle. The fracture energies of the 10% blend increased slightly with clamp speed up to 1 m s^{-1}, at 10 m s^{-1} slightly lower but still ductile. The fracture energies of the 45% blend seem to be insensitive to the test speed, even at 10 m s^{-1}. The advantage of 10 and 45% blends compared to PC is that they fractured ductile over the whole studied test speed range. It can also be expected that the 45% blend compared to the 10% blend has a lower brittle-to ductile transition temperature. The general trend is that addition of ABS lowers the brittle–ductile transition temperature (T_{bd}) although it lowers the fracture stress, does not lead to a higher fracture strain and lowers the fracture energies.

The PC/ABS blend containing 10% ABS was investigated further. SENT tests were done at different temperatures over the complete test speed range (Fig. 3).

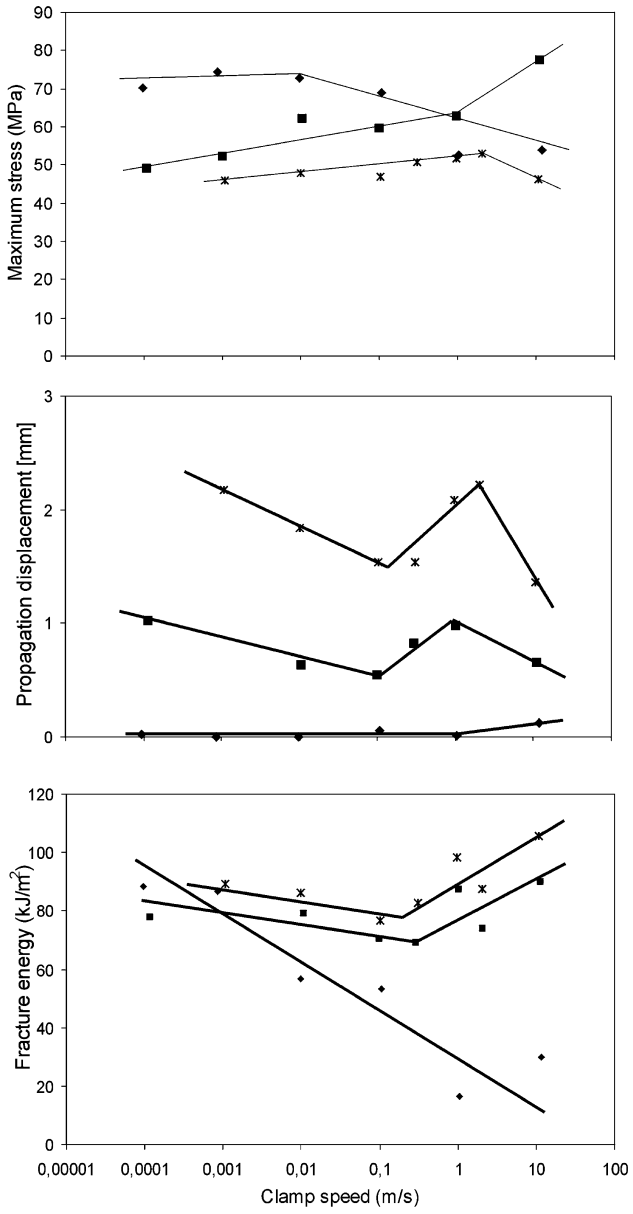

Fig. 3. Influence of test speed on SENT results (maximum stress, fracture propagation displacement, and fracture energy) for dispersed PC/ABS blend (type I, 90/10) at different temperatures: (◆) −60 °C; (■) 20°C; (∗) +60 °C.

At −60 °C, brittle fracture occurred at all test speeds and the maximum stress decreased with test speed (Fig. 3a). At this temperature, the brittleness increased at increasing test speeds. At 20 °C ductile fracture occurred and maximum stress now increased with test speed, as discussed earlier. The values were also higher that those at −60 °C, which suggest that the yield stress was reached here. At 60 °C the maximum stress values were fairly independent of test speed and lower than those at 20 °C. The values at 60 °C are yield values too, and since the temperature is higher, the yield stress is lower.

Of the fracture displacement the propagation displacement

is shown (Fig. 3b). The propagation displacement is a measure for additional deformation in the sample during crack propagation. The propagation displacement shows a strong effect on both temperature and test speed. At −60 °C the propagation displacement is minimal over the whole test speed range, which means that here this material fractures in a brittle manner. At 20 °C the propagation displacement results are complex. The values first decreased with increasing test speed, up to about 0.1 m s^{-1} test speed, then jumps to a higher level and decreased again with further increase in test speed. A similar complex behaviour is observed with the 60 °C values. The high strain rate values for the 20 and 60 °C results cannot be explained by extrapolation of the low strain rate values. It seems as if at high strain rates the crack propagation process is different from that at low strain rates. The 60 °C displacement values are higher than those at 20 °C. This is logical since at 60 °C the yield stress is lower.

The fracture energy at −60 °C decreases steadily with strain rate (Fig. 3c). The 20 °C values seem to be fairly constant up to 0.3 m s^{-1} and increased at higher test speeds. The 60 °C values decreased up to 0.1 m s^{-1} and increased at high strain rates. The fracture energies are now also larger than those at 20 °C. The energy levels for the 20 and 60 °C tests at high speeds were even higher than those at low speeds. Test speed apparently affects the deformation process.

The brittle-to-ductile transition temperature (T_{bd}) was studied for the dispersed PC/ABS (90/10) blend as a function of test speed (Fig. 4). The T_{bd} was determined from propagation displacement results and the fracture surface appear.

At low speeds the transition from brittle to ductile was gradual. The first signs of ductility could be seen on the fracture surface just behind the notch. With increasing temperature the whole fracture surface becomes 'ductile'. The temperature range in which this transition took place decreased with strain rate. In this transition zone the running crack seemed to accelerate due to the release of elastic energy stored in the crack initiation phase [13]. Here T_{bd} is defined as the onset of ductile deformation.

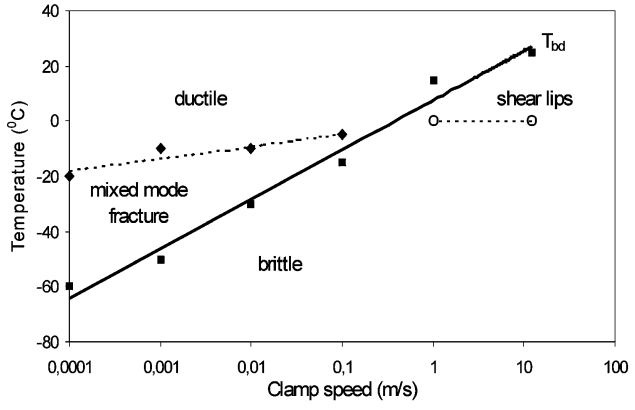

Fig. 4. Influence of test speed on transition temperatures for PC/ABS (90/10 blend): (■) T_{bd}; (◆) temperature below which mixed mode fracture occurs, and above which shear lips can form.

At high speeds, with increasing temperature, the first ductile signs were shear lips that formed along the specimen surface. The plane stress situated at the specimen surface enables the material to yield sooner than the material at the core of the specimen. At a higher temperature, the material in the middle of the sample behind the notch fractures also in a ductile manner. The T_{bd} is here also taken as when the material behind the notch in the middle of the sample fractures ductile. So over the studied test speed range the T_{bd} increases linearly with the logarithm of the test strain rate ($\log \dot{\varepsilon}$) (Eq. (3)). The pre-exponential factor A had a value of 18.6.

$$\Delta T_{bd} = A \log \dot{\varepsilon} \tag{3}$$

No unusual effects at high test speeds were observed. The T_{bd} increase with test speed is the same as observed for PC [13]. However, for PC the shear lip effect was not observed.

The effects of test speed on maximum stress, fracture displacement, and fracture energy suggest a special effect at high test speeds. Similar effects were also found for PP–rubber blends [10] and SAN–rubber blends [12], though more pronounced than for the PC/ABS material. These strain rate effects in modified PP and SAN were attributed to a thermal blunting process during crack propagation, as a result of temperature increase in the zone ahead of the crack tip. The brittle–ductile transition for PC/ABS however increased steadily with test speed. This suggests that the brittle–ductile transition is not influenced by a thermal blunting process. The increased fracture energies at high strain rates are as yet not fully understood.

3.2. Co-continuous PC/ABS

The co-continuous PC/ABS blend (50/50) (Blend II), where ABS contained 15% PB, had a T_{bd} of −15 °C in notched Izod [14]. In a SENT test at 1 m s^{-1} and room temperature this blend fractured in a ductile manner. The influence of strain rate is now studied over the speed range of 10^{-4}–10 m s^{-1} at room temperature (Fig. 5). With a specimen length between the clamps of 35 mm, this results in initial strain rates of 2.85×10^{-3}–285 s^{-1}.

The maximum stress in the SENT test increased with test speed (Fig. 5a), especially for high clamp speeds. This effect was also found for PC and PC/ABS with dispersed ABS (Fig. 2), and is stronger than can be expected based on Eyring Eq. (1). The yield stress of PC as measured in a tensile test increases with strain rate and particular at high strains [15], although not so strong as the maximum stress in SENT (Fig. 5a). For PP the influence of strain rate on the yield strength was stronger than for PC [10]. A high maximum stress in SENT at high strain rates was also observed in PA, PP, and SAN-blends [9,10,12].

The clamp displacement needed to fracture the specimen is measured in the SENT tests (Fig. 5b). This fracture

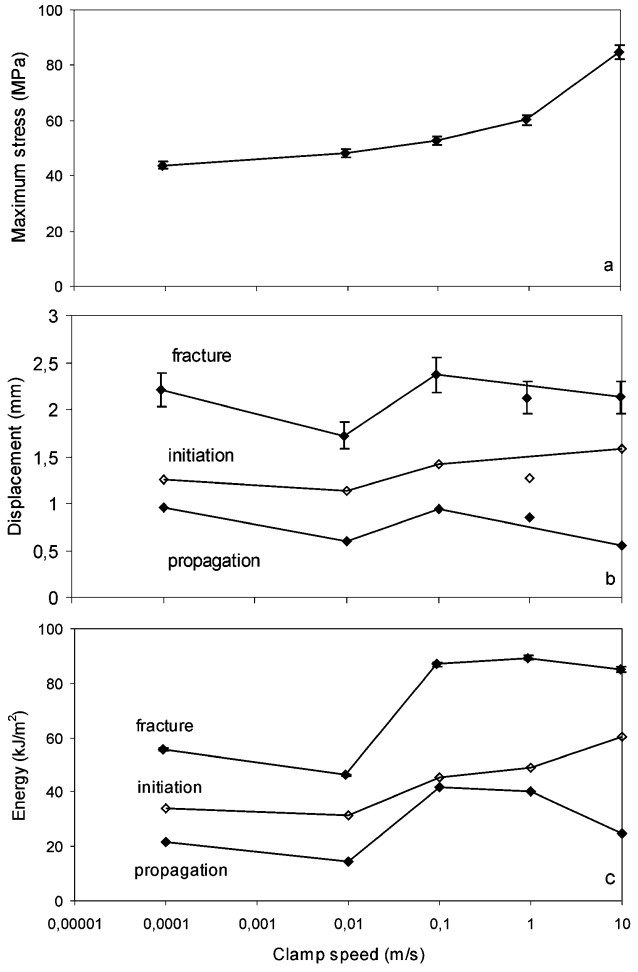

Fig. 5. Influence of test speed on SENT results (maximum stress, displacement, and energy), co-continuous PC/ABS (Type II, 50/50) 15% PB in ABS, at room temperature.

displacement was not gradually lowered with strain rate as expected but increased even at clamp speed of 0.1 m s^{-1} and higher.

Displacement results were split into an initiation and propagation part. Initiation displacement increased with increasing strain rate, which means a more ductile behaviour with increasing strain rate. The propagation results decreased first, then showed a jump at 0.01–0.1 m s^{-1} and decreased again at higher test speeds. These results of the co-continuous blend have a similar behaviour in this respect as the dispersed blends (Fig. 3). A decreasing propagation displacement is not unexpected since at higher speeds the material behaves more brittle. However, the higher propagation displacements at higher test speeds suggest a change in deformation process. A possible explanation for this effect is adiabatic heating [9,10].

The results for the deformation energies (Fig. 5c) showed the same trends as for the displacement results (Fig. 5b) but more clearly. The maximum in fracture energy could be completely attributed to the maximum in propagation energy. Initiation energy increased gradually from 0.01 m s^{-1}, as did the maximum stress. Due to this increase in initiation energy, fracture energy was very high at high test speeds, even higher than low speed fracture energy.

Comparing fracture energies for co-continuous PC/ABS (Fig. 5c) with PC and dispersed PC/ABS (Fig. 2c), we see that the co-continuous blend has a lower fracture energy than PC in the ductile region, and compares with that of dispersed PC/ABS. However, the transition from ductile to brittle fracture occurs at a much lower temperature for co-continuous PC/ABS than for PC and dispersed PC/ABS [14].

The stress-whitened zone below the fracture surface had a maximum thickness of about 3 mm and this is for all test speeds. At high test speeds, the fracture surface shows a delamination structure, as was found in the notched Izod impact tests [14]. In the fracture surface with the size of 4×8 mm^2, 2–3 circular (onion like) cracks are visible which have a depth of about 1–2 mm. Failure of the layered PC/ABS interface leads to the appearance of this feature on the fracture surface. Delamination was observed just above the brittle to ductile transition temperature and disappeared at high temperatures and high rubber contents [14]. The plain strain stress state was assumed to be less severe under the latter conditions. Delamination was not observed in dispersed PC/ABS blends.

Delamination was also influenced by test speed. With increasing test speed, delamination developed, at least as long as the fracture was ductile and at the same time the propagation energy and propagation displacement increased. However, it is the question whether this increase in propagation energy and propagation displacement is due to the delamination?. With ABS dispersed in PC, we did not see delamination, although there the fracture energy and propagation displacement increased with test speed too. This suggests that the delamination does not contribute to the fracture energy and propagation displacement. The high fracture displacements and fracture energies at high test speeds of the co-continuous blend might therefore be attributed to adiabatic heating. An adiabatic heating effect has been previously suggested for ABS and other polymers [9,10,12]. It is evident that at high strain rates the fracture energy of PC/ABS is higher than can be expected from the low strain rate data.

3.2.1. Infrared temperature measurements

Strong deformations at high test speeds are expected to increase the temperature of the deformation zone. To obtain an indication of the temperature rise in the deformation zone ahead of the notch tip, an infrared camera was used to monitor the temperature development during SENT tests at different test speeds. The used infrared camera takes 30 frames s^{-1}. For lower test speeds, the fracture process can be monitored completely. For test speeds of 0.1 m s^{-1} and higher, fracture of the specimen is fast and takes place in the interval between two frames. With this camera, having a

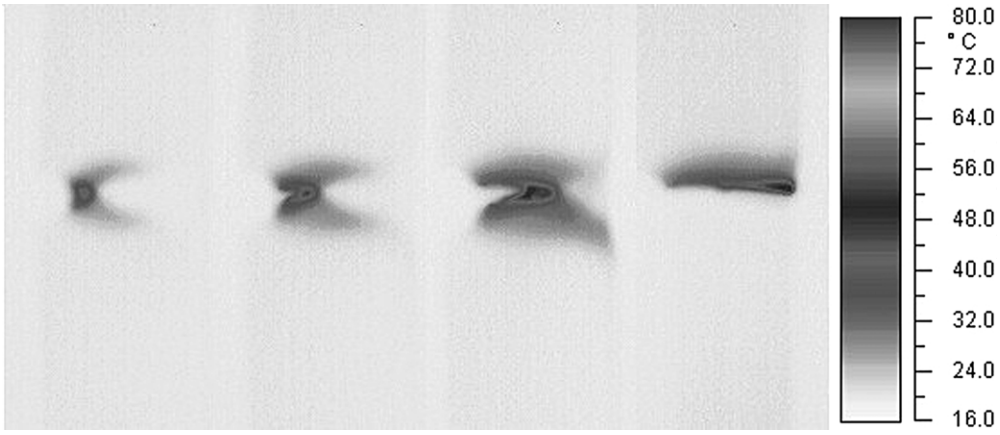

Fig. 6. Temperature effects of PC fracture in SENT tested at 10^{-3} m s^{-1} and at room temperature.

spot size of 100 μm, the temperature very near the fracture surface (1–20 μm) could not be determined.

Frames of fracture at 10^{-3} m s^{-1} are shown for PC in Fig. 6. The specimens showed far from the notch zone a small rise in overall temperature of a few degrees, indicating that also outside the notch zone some plastic deformation occurs. This rise in temperature outside the notch zone did not change with test speed. The deformation zone was concentrated into two lobes, located symmetrically along the fracture plane. These lobes are somewhat smaller at higher test speeds. Just ahead of the notch, a zone was visible where temperature was higher. The point of highest temperature in the deformation zone was located at some distance ahead of the notch or running crack. The infrared images showed also clearly that a running notch in a ductile mode was less sharp than the machined notch and thus blunting was taking place during fracture.

For the co-continuous PC/ABS blend heating pattern similar to PC was seen (Fig. 7). The size of the zone of increased temperature (deformation zone) seen ahead of the notch appeared for co-continuous PC/ABS to be somewhat less extensive than for the pure PC specimens. This agrees with the lower fracture energies found for co-continuous PC/ABS compared to pure PC.

The maximum measured temperatures increased slightly with test speed for PC and PC/ABS, from 45 to a maximum of 55 °C (Fig. 8). These temperatures are much lower than the T_g of the SAN (120 °C) or the PC phase (150 °C). The effect of speed on temperature is not strong and much less than that observed for PP and rubber modified PP [10].

The test speed seems to increase the zone size (Fig. 9). This is remarkable, as one would expect normally a decrease in deformation zone size with increasing strain rate.

The observed increase in temperature leads to a decrease in drawing stress and more yielding can take place. More plastic deformations in the notch blunts the notch and even more yielding can take place. This deformation being a self-amplifying process can result in a delocalisation of the deformation ahead of a running crack and higher energy absorption during fracture of the material. In the layer next to the fracture surface (0–20 μm thick) the deformation is usually stronger than further away, but the temperature there can unfortunately with this method not be measured.

4. Conclusions

The maximum stresses, the fracture propagation

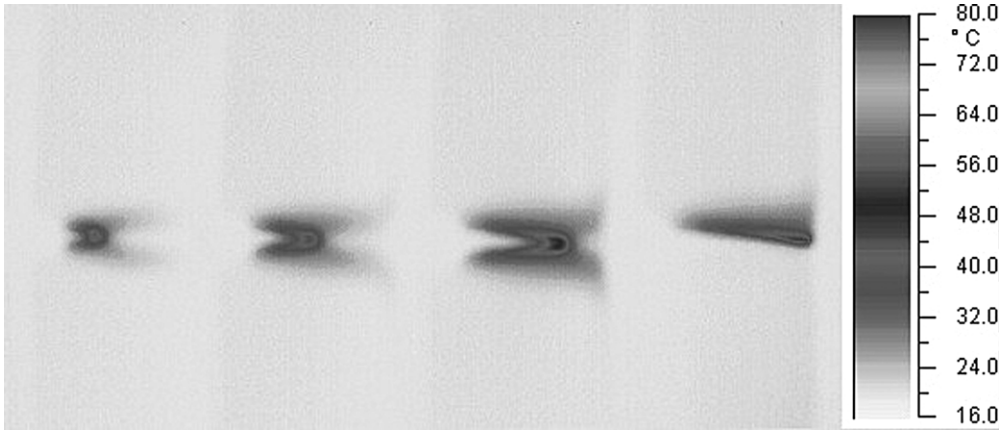

Fig. 7. Temperature effects of co-continuous PC/ABS fracture in SENT tested at 10^{-3} m s^{-1} and at room temperature.

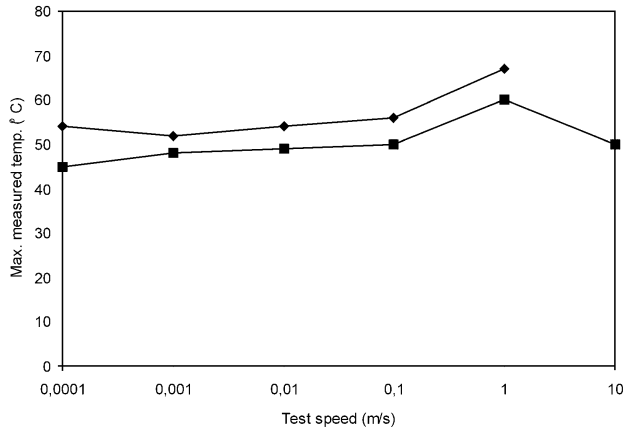

Fig. 8. Influence of test speed on maximum temperature measured during SENT tests at room temperature, (◆) PC; (■) PC/ABS (50/50).

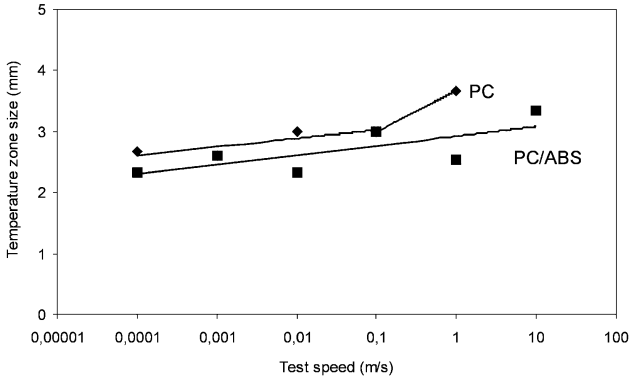

Fig. 9. Influence of test speed on size of the temperature zone for PC (◆), and co-continuous PC/ABS (■).

displacements and the fracture energies at high strain rates were higher than was expected based on low strain rate results. Also the size and the temperature of the deformation zone increased with strain rate. This suggests that at high test speeds a more delocalised deformation process is taking place. This delocalisation might well be the result of either lowering of drawing stress due to the increased temperature and/or notch/crack blunting. The blunting of the notch results in a reduction of the constraint ahead of the tip, leading to more deformation and more material taking part in the deformation. The rate effect was somewhat larger for PC than for co-continuous PC/ABS blend. Since notch tip radius has a stronger effect on the toughness of PC than on PC/ABS blends [16], toughness of PC will also be more affected by notch blunting. Looking into more details of the fracture propagation displacement data, at high strain rates a change in fracture process seems to take place.

Infrared measurements of the temperature rise during SENT testing showed that the temperature in the deformation zone ahead of the notch increased. The observed temperature rise was limited and the glass transition temperature of either PC or SAN was not reached. However, the temperature directly at the fracture surface could not be determined with the camera having a spot size of 100 μm. The rise in temperature of the material ahead of the notch and crack must have an effect on the deformation behaviour.

The strain rate had a strong effect on the brittle–ductile transition temperature. The T_{bd} increased linearly with the logarithm of the strain rate by a factor of 18.6. At high test speeds no deviation was observed from this trend. This suggests that thermal blunting can have an effect on ductile fracture, but not on the brittle–ductile transition.

Acknowledgements

This work was sponsored by FOM, Fundamental Materials Research Program of the Netherlands. The authors would like to thank Prof. L.C.E. Struik, Prof. E. van der Giessen and R.G. van Daele at DOW Benelux for their support and stimulating discussions.

References

[1] Bucknall CB. Polymer blends. New York: Wiley, 2000. Chapter 22.
[2] Roetling JA. Polymer 1965;6:311.
[3] Ishai O, Cohen L. J Compos Mater 1986;2:301.
[4] van der Wal A, Gaymans RJ. Polymer 1999;40:6045–55.
[5] Gaymans RJ, Dijkstra K. Impact and dynamic fracture of polymers and composites, ESIS 19. Williams JG, Pavan A, editors. Mech Engng Lond 1995:191–201.
[6] Williams JG, Hodgkinson JM. Proc R Soc Lond 1981;A375:231–48.
[7] Marshall GP, Coutts LH, Williams JG. J Mater Sci 1974;9:1409–19.
[8] Weichert R, Schönert K. J Mech Phys Solids 1974;22:127.
[9] Dijkstra K, ter Laak J, Gaymans RJ. Polymer 1994;35(2):2315–22.
[10] van der Wal A, Gaymans RJ. Polymer 1999;40:6045–55.
[11] Ricco T, Pavan A. Angew Makromol Chem 1992;201:23–31 (Nr. 3496).
[12] Steenbrink AC, Gaymans RJ, van der Giessen E. Polymat'94, London, UK; 19–22 September. p. 598–601.
[13] Gaymans RJ, Hamberg MJJ, Inberg JPF. Polym Engng Sci 2000;40(1):256–62.
[14] Inberg JPF, Gaymans RJ. Polymer, co-continuous PC–ABS blend. In press.
[15] Yee AF. J Mater Sci 1977;12:757–65.
[16] Inberg JPF, Gaymans RJ. Polycarbonate and co-continuous polycarbonate/ABS blends: influence of notch radius. Submitted for publication.